



Title	Influence of arsenic stress on synthesis and localization of low-molecular-weight thiols in <i>Pteris vittata</i>
Author(s)	Sakai, Yuki; Watanabe, Toshihiro; Wasaki, Jun et al.
Citation	Environmental Pollution, 158(12), 3663-3669 https://doi.org/10.1016/j.envpol.2010.07.043
Issue Date	2010-12
Doc URL	https://hdl.handle.net/2115/44315
Type	journal article
File Information	EP158-12_3663-3669.pdf



Influence of arsenic stress on synthesis and localization of low-molecular-weight thiols in *Pteris vittata*

Yuki Sakai ^{a,1}, Toshihiro Watanabe ^{a,*}, Jun Wasaki ^b, Takeshi Senoura ^c, Takuro Shinano ^d, Mitsuru Osaki ^a

^a Research Faculty of Agriculture, Hokkaido University, Kita 9, Nishi 9, Kitaku, Sapporo 060-8589, Japan

^b Graduate School of Biosphere Science, Hiroshima University, Kagamiyama 1-7-1, Higashi-Hiroshima 739-8521, Japan

^c Graduate School of Agricultural and Life Sciences, The University of Tokyo, 1-1 Yayoi, Bunkyo-ku, Tokyo 113-8657, Japan

^d National Agricultural Research Center for Hokkaido Region, Sapporo 062-8555, Japan

¹ Present address: Fujita Co., 2025-1 Ono, Atsugi, Kanagawa 243-0125, Japan

* Author for correspondence: Dr Toshihiro Watanabe

Research Faculty of Agriculture, Hokkaido University, Kita 9, Nishi 9, Kitaku, Sapporo 060-8589, Japan

Tel: +81-11-706-3845

Fax: +81-11-706-3845

Email: nabe@chem.agr.hokudai.ac.jp

Abstract

The roles of low-molecular-weight thiols (LMWTs), such as glutathione and phytochelatins, in arsenic (As) tolerance and hyperaccumulation in *Pteris vittata* an As-hyperaccumulator fern remain to be better understood. This study aimed to thoroughly characterize LMWT synthesis in *P. vittata* to understand the roles played by LMWTs in As tolerance and hyperaccumulation. LMWT synthesis in *P. vittata* was induced directly by As, and not by As-mediated oxidative stress. Expression of *PvECS2*, one of the putative genes of γ -glutamylcysteine synthetase (γ ECS), increases in *P. vittata* shoots at 48 h after the onset of As exposure, almost corresponding to the increase in the concentrations of γ -glutamylcysteine and glutathione. Furthermore, localization of As showed similar trends to those of LMWTs in fronds at both whole-frond and cellular levels. This study thus indicates the specific contribution of LMWTs to As tolerance in *P. vittata*. γ ECS may be responsible for the As-induced enhancement of LMWT synthesis.

Capsule: *Pteris vittata* specifically enhances low-molecular-weight thiol synthesis against arsenic toxicities

Keywords: arsenic tolerance, low-molecular-weight-thiol, *Pteris vittata*, γ -glutamylcysteine synthetase, oxidative stress

1. Introduction

It is believed that arsenate [As(V)], the dominant inorganic species of arsenic (As) in upland soils (Francesconi et al., 2002), enters the root cells via phosphate transporters because As(V) is a chemical analogue of phosphate (Caille et al., 2004; Kertulis et al., 2005). In higher plants, absorbed As(V) is rapidly reduced to As(III) by As(V) reductase (Bleeker et al., 2006) or nonenzymatically by glutathione (GSH) (Delnomdedieu et al., 1994). As(III) reacts with the thiol groups (-SH) of proteins in plant tissues leading to inhibition of cellular function and, ultimately, death (Ullrich-Eberius et al., 1989). In addition to these direct toxicities, the role of As-induced oxidative stress in As toxicity in plants has also been suggested (Requejo and Tena, 2005).

It is known that higher plants exposed to As show a substantial increase in low molecular-weight thiols (LMWTs), such as cysteine (Cys), γ -glutamylcysteine (γ EC), GSH, and phytochelatins (PCs), which form complexes with As(III) resulting in inactivation of As in the plant (Grill et al., 1985; Srivastava et al., 2010). The -SH groups of these LMWTs are responsible for binding to As(III). Among these LMWTs, GSH and PCs, oligomers of GSH, are regarded as major ligands for As(III). Furthermore, LMWTs also contribute in alleviating oxidative stress induced by As (Shri et al., 2009). Thus, LMWT synthesis plays a crucial role in mechanisms of As tolerance. Many studies have focused on the LMWT synthesis pathway to investigate the mechanisms of As tolerance in higher plants. Previous attempts to enhance As tolerance by overexpressing the genes involved in

production of enzymes responsible for LMWT synthesis thus contributing to an increase in the LMWT pool (Li et al., 2006; Dhankher et al., 2002) are an example. In particular, γ EC synthetase (γ ECS) is often targeted because γ EC synthesis is a rate-limiting factor in the LMWT synthesis pathway (Tripathi et al., 2007).

Pteris vittata L. (Chinese brake fern) is the first fern to be identified as an As hyperaccumulator (Ma et al., 2001). This species accumulates more than 10,000 mg As kg⁻¹ dry weight in their shoots (Wang et al., 2002) as compared with 40 mg As kg⁻¹ in most plant species (Watanabe et al., 2007). Thus, *P. vittata* can accumulate extremely high levels of As, but the mechanisms of As absorption and translocation as well as those for As tolerance remain to be elucidated. Its high tolerance suggests the possibility of As detoxification in the form of As(III)-LMWT complexes in shoots, as in higher plants, but more effectively. Actually, Vetterlein et al. (2009) reported the significant positive correlation between As and total sulfur in fronds of *P. vittata*. However, Zhao et al. (2003) reported a limited role of PCs in the detoxification of As(III) *P. vittata* because of a low PC-SH to As molar ratio of (0.09–0.03). In addition, Raab et al. (2004) detected an extremely low proportion of As(III) as PCs complexes in *P. cretica*. Pickering et al. (2006) demonstrated that most As in *P. vittata* is in an inorganic form using x-ray absorption near-edge structure (XANES). Meanwhile, an unknown thiol was identified in *P. vittata* (Zhang et al., 2004; Cai et al., 2004).

Thus, the roles of LMWTs in the mechanism of As tolerance in *P. vittata* are uncertain. This study

aims to examine the impact of As stress on LMWT synthesis and distribution in *P. vittata*.

2. Materials and Methods

2.1. Experiment 1: Arsenic-induced changes in low-molecular-weight thiol synthesis in *Pteris vittata* and *Nephrolepis exaltata*

2.1.1. Plant materials

Seedlings of *P. vittata* were kindly supplied by Fujita Corporation (Tokyo, Japan). Seedlings of *N. exaltata* a nonhyperaccumulator fern were purchased from a garden center. The seedlings were cultivated in peat moss prior to experimentation. Roots were washed carefully with tap water to remove adhering soil and then seedlings uniform in shoot height (ca. 10 cm) were transferred to continuously aerated 4-L pots (three seedlings per pot) containing a nutrient solution for preculture in hydroponics. The standard nutrient solution contained 2.14 mM N (NH_4NO_3), 32 μM P ($\text{NaH}_2\text{PO}_4 \cdot 2\text{H}_2\text{O}$), 0.77 mM K (K_2SO_4 : KCl = 1 : 1), 1.25 mM Ca ($\text{CaCl}_2 \cdot 2\text{H}_2\text{O}$), 0.82 mM Mg ($\text{MgSO}_4 \cdot 7\text{H}_2\text{O}$), 35.8 μM Fe ($\text{FeSO}_4 \cdot 7\text{H}_2\text{O}$), 9.1 μM Mn ($\text{MnSO}_4 \cdot 4\text{H}_2\text{O}$), 46.3 μM B (H_3BO_3), 3.1 μM Zn ($\text{ZnSO}_4 \cdot 7\text{H}_2\text{O}$), 0.16 μM Cu ($\text{CuSO}_4 \cdot 5\text{H}_2\text{O}$), and 0.05 μM Mo [$(\text{NH}_4)_6\text{Mo}_7\text{O}_{24} \cdot 4\text{H}_2\text{O}$]; total $\text{SO}_4 = 1.06$ mM. The solution pH was adjusted daily to 5.3–5.5 and was renewed once a week. Plants were grown in hydroponic culture in a greenhouse at Hokkaido University (13–15 h photoperiod and day/night temperature of 25–28/18–22°C) for 3–4 weeks until new roots developed.

2.1.2. Arsenic exposure

Seedlings of *P. vittata* and *N. exaltata* were exposed to 0, 100, and 500 μM As(V) (supplied as Na_2HAsO_4) in a standard nutrient solution. The plants were harvested and rinsed with deionized water after three days of exposure, and separated into shoots and roots. The samples were lyophilized and concentrations of As and LMWTs were determined. Each treatment was performed in triplicate.

2.1.3. Arsenic analysis

A total of 10 mg of lyophilized samples and 1.5 mL of 61% HNO_3 (EL grade, Kanto Chemical, Tokyo) were heated together at 110 $^\circ\text{C}$ in a DigiPREP apparatus (GL Science, Tokyo) for ca. 2 h until the most of the solution evaporated. Following this, 0.5 mL H_2O_2 (semiconductor grade, Santoku Chemical, Tokyo) was added, and the sample was heated at 110 $^\circ\text{C}$ for another 15–20 min. The digestion tube was filled with 2% HNO_3 to make 20 mL. Arsenic concentration was determined by using ICP-MS (ELAN DRC-e, Perkin Elmer, Waltham, MA, USA).

2.1.4. Extraction and analysis of low-molecular-weight thiols

The concentrations of Cys, γEC , and GSH in the plants were measured using a modification of the methods of Sneller et al. (2000) and Zhao et al. (2003). Lyophilized plant samples (10 mg) were ground on ice using a mortar and pestle in 2 mL extraction solution [6.3 mM diethylene-triamine pentaacetic acid (DTPA) with 0.1% trifluoroacetic acid (TFA)]. A preliminary experiment indicated

that the frond midribs interfered with the extraction process and subsequently inhibited the detection of LMWTs (Fig. S1). Hence, the midrib was removed in most experiments in this study, even when measuring LMWTs in fronds. The extraction solution contained 1 mg L^{-1} N-acetyl L-cysteine as an internal standard. The extracts were centrifuged at $13,000 \text{ g}$ for 10 min at $4 \text{ }^{\circ}\text{C}$, and the supernatant was filtered through $0.22 \text{ }\mu\text{m}$ membrane filters. Then, $250 \text{ }\mu\text{L}$ of this extract together with $450 \text{ }\mu\text{L}$ of a derivatization buffer [200 mM 4-(2-hydroxyethyl)-piperazine-1-propanesulfonic acid and 6.3 mM DTPA at $\text{pH } 8.2$] was derivatized with $10 \text{ }\mu\text{L}$ of 25 mM monobromobimane. Derivatization was carried out at $45 \text{ }^{\circ}\text{C}$, for 30 min in the dark, and the reaction was stopped by adding $300 \text{ }\mu\text{L}$ of 1 M methyl sulfonic acid. The derivatized sample was stocked at $4 \text{ }^{\circ}\text{C}$, in the dark until HPLC analysis. LMWTs were separated using an HPLC column [TSK gel-ODS 80Ts ($3.9 \times 300 \text{ mm}$), TOSO, Tokyo] at $37 \text{ }^{\circ}\text{C}$, and fluorescence was monitored using a fluorescence detector (FP2020, Jasco, Tokyo) with excitation and emission wavelengths of 380 and 470 nm , respectively. The following mobile phases were used: eluent A, water with 0.1% TFA; and eluent B, methanol with 0.1% TFA. A linear gradient was performed from eluent B in different concentrations; 12% at 0 min , 25% at 15 min , 35% at 29 min , and 50% at 50 min .

2.2. Experiment 2: Relationships between various oxidative stresses and low-molecular-weight thiol synthesis in Pteris vittata

2.2.1. Treatment

Seedlings of *P. vittata* were treated with or without various stressors: 100 μM As(V) (supplied as Na_2HAsO_4), 50 μM cadmium (supplied as CdCl_2), or 1 mM H_2O_2 . These three stressors are known to induce oxidative stress (Hartley-Whitaker et al., 2001; Benavides et al., 2005; Schützendübel et al., 2002). The plants were harvested at 0, 1, 2, and 3 days after initiating the treatment. The samples were rinsed with deionized water, and separated into shoots and roots. A part of the fresh root samples was used for analysis of lipid peroxidation, while the rest was lyophilized for LMWT analysis. Concentrations of LMWTs were determined as described in Experiment 1.

2.2.2. Determination of lipid peroxidation

Lipid peroxidation in roots was estimated by measuring the amount of thiobarbituric acid reacting substance (TBARS) (Singh et al., 2006). Fresh plant tissue samples (0.5 g) were cut into small pieces, homogenized using a mortar and pestle on ice with 2.5 mL of 5% trichloroacetic acid, and centrifuged at 10,000 g for 15 min at room temperature. Equal volumes of supernatant and 0.5% thiobarbituric acid in 20% trichloroacetic acid were added to a new tube and incubated at 96 °C for 25 min. The tubes were immediately put on ice following incubation, and then centrifuged at 8,000 g for 5 min. The absorbance of the resulting supernatant was recorded at 532 nm and corrected for

nonspecific turbidity by subtracting the absorbance at 600 nm. The concentration of TBARS was then calculated using an extinction coefficient of $155 \text{ mM}^{-1} \text{ cm}^{-1}$.

2.3. Experiment 3: Expression analysis of arsenic related genes in *Pteris vittata*

2.3.1. Cloning of putative γ -glutamylcysteine synthetase gene in *Pteris vittata* (*PvECS*)

Lyophilized shoot samples of *P. vittata* seedlings grown with $100 \mu\text{M As(V)}$ for 3 days were ground to a fine powder over liquid nitrogen. Total RNA was extracted from the samples using a Total RNA Isolation Mini Kit (Agilent Technologies, Santa Clara, CA), of which $0.5 \mu\text{g}$ was reverse-transcribed into cDNA using a SuperScript III First-strand Synthesis for Reverse Transcription (RT)-PCR Kit (Invitrogen, Carlsbad, CA). The amino acid sequences of γECS have already been identified in various plants, including *Arabidopsis thaliana*, *Brassica juncea*, and *Oryza sativa*. Two primers, 5'-ATHGGNACNGARCAYGARAAR-3' (forward) and 5'-ACRAARTACATNGGNACRTCNR-3' (reverse), were designed on the conserved amino acid sequences from the NCBI database for RT-PCR. PCR amplification was run on the cDNA from *P. vittata*. PCR conditions were 2 min at $94 \text{ }^\circ\text{C}$, 35 cycles of 30 s at $94 \text{ }^\circ\text{C}$, 30 s at $46 \text{ }^\circ\text{C}$, and 1 min at $72 \text{ }^\circ\text{C}$, followed by 5 min at $72 \text{ }^\circ\text{C}$. The 600 bp fragment was cloned and sequenced, and the partial sequence was extended toward the 5' and 3' ends by rapid amplification of cDNA ends (RACE).

To extend the *PvECS* gene sequence in the 5'- and 3'-directions, the RACE reaction was

performed using a 3'- and 5'- Full RACE Core Sets (Takara Bio, Otsu, Japan). The 3'-RACE reaction was carried out according a per the following protocol: 2 min at 96 °C, 30 cycles of 10 s at 98 °C, 10 s at 55 °C, and 1 min at 72 °C, followed by 2 min at 72 °C using the gene specific primer: 5'-CCTTACAG CCTATTGCAACCGC-3' and 3' site adaptor primer. Nested amplification was performed under the same conditions, using an adaptor primer and a gene specific primer: 5'-TCTTCCATG AAGATTTTGGGTTTGAG-3'. For the 5'-RACE reaction, the PCR primer was based on the fragments obtained from the RT-PCR. Primary amplification was carried out using the gene specific primers: 5'-CGTGTCCCTGGAGCCTGGTG-3' (forward) and 5'-GCCATCCTGTGTTAATCCAATGATC-3' (reverse) under the following PCR conditions: 2 min at 94 °C, 30 cycles of 20 s at 94 °C, 30 s at 50 °C, and 1 min at 72 °C, followed by 2 min at 72 °C. Nested amplification was performed under the same PCR conditions using the primers: 5'-CTCAGTGGTGCTCCTCT TGAGAC-3' (forward), and 5'- GTCTCTTCCAATTAACGCTC TGC-3' (reverse).

2.3.2. Arsenic Treatment

Seedlings of *P. vittata* were precultured as described above, transplanted to a standard nutrient solution containing 100 µM As(V) with continuous aeration, and harvested at 0, 0.5, 1, 5, 12, 24, 48, and 72 h after the onset of the As exposure. After harvesting, the plants were separated into shoots and roots, and rinsed with deionized water. The shoots and roots were used for gene expression as

well as LMWT and As analyses. Concentrations of LMWTs and As were determined as described in Experiment 1.

2.3.3. Real-time PCR

Real-time PCR was carried out using a Smart Cycler II System (Cepheid, Sunnyvale, CA) and SYBR Premix Ex Taq (Takara Bio, Otsu, Japan). Total RNA was extracted from the shoot and root of *P. vittata*, and treated with DNase to remove template DNA. After the DNase treatment, RNA samples were reverse-transcribed into cDNA using SuperScriptIII First-Strand Synthesis System for RT-PCR Kit (Invitrogen, USA). The target genes were the γ ECS genes (*PvECS1* and *PvECS2*) in shoots, and PC synthase (*PvPCS*) as well as As(V) reductase genes (*PvACR2*) in shoots and roots. The elongation factor gene (*PvEF-1b*) was used as an endogenous control because its expression was relatively stable (Ellis et al., 2006). The gene specific primers were 5'-GTAGATCCTGTCTATGAAGAGCTC-3' (forward) and 5'-GAACTCAGACTCTCCAGGAATG-3' (reverse) for *PvECS1*, 5'-TTTATTGGATTGCTTGGCAAAGAGGC-3' (forward) and 5'-GTTCAATCATTAAGAATGGATGGTGC-3' (reverse) for *PvECS2*, 5'-GCAAGTATCTGGTGGGCAAG-3' (forward) and 5'-GGGATGTGTTGACTGATGAG-3' (reverse) for *PvPCS* (Dong et al., 2005), and 5'-GCATAGCGGACCTGCATGT-3' (forward) and 5'-GCGGCTTCGATTTCTTTCTTG-3' (reverse) for *PvACR2* (Ellis et al., 2006), and

5'-CAACAGTATCGTGCTCGACTCT-3' (forward) and 5'-GGCAATGCGTAACCCTCATAA-3' (reverse) for *PvEF-1b* (Ellis et al., 2006).

2.4. Experiment 4: Localization of arsenic and low-molecular-weight thiols

2.4.1. Localization in segmentalized frond

P. vittata seedlings were exposed to 100 μ M As(V) in standard nutrient solution with continuous aeration for 3 days. After exposure, the shoot was separated into veins and other parts in each pinna. The pinna located at the apical position was further separated into three parts: vein, edge of pinna, and central parts of pinna. After segmentalization, these samples were immediately frozen in liquid nitrogen and lyophilized. The As and LMWT concentrations in each segment were determined as described above. In this experiment, PC₂ ((γ Glu-Cys)₂-Gly) was measured in addition to Cys, γ EC, and GSH. The PC₂ standard was synthesized by Shimadzu Corporation (Kyoto, Japan).

2.4.2. Cellular localization of glutathione

P. vittata exposed to 100 μ M As(V) for 5 days were stained for GSH. The apical pinna and root were washed with Tris-HCl buffer (pH 8.5). Cross sections (30 μ m) of the apical pinna and root were cut with a cryostat (CM-3000; Leica Microsystems, Wetzlar, Germany), and placed on slides. Cellular localization of GSH was determined using the fluorescence probe monochlorobimane (MCB). The reaction of MCB with GSH is catalyzed by glutathione-S-transferase to form a blue

fluorescent GSH-bimane complex. The sections on the glass slides were covered with 1 mM MCB solution in Tris-HCl buffer (pH 8.5) for 30 min in the dark at room temperature to stain GSH. After staining, the sections were washed three times with Tris-HCl buffer. The GSH-bimane complex in the section was observed under a fluorescence microscope (Leica FW 4000, Leica Microsystems, Wetzlar, Germany) with excitation and emission wavelengths of 434 and 477 nm, respectively.

2.5. Statistics

The results were analyzed using ANOVA and Tukey's multiple comparison test in instances of significant treatment effects ($P < 0.05$).

3. Results

3.1. Experiment 1: Arsenic-induced changes in low-molecular-weight thiol synthesis in *Pteris vittata* and *Nephrolepis exaltata*

P. vittata and *N. exaltata* were exposed to two different levels of As (100 and 500 μ M) for three days. No toxicity symptoms were observed in both *P. vittata* and *N. exaltata* after exposure. In shoots, the concentration of As was higher in *P. vittata* than in *N. exaltata* (Fig. 1). In contrast, *N. exaltata* roots showed higher concentrations of As. The shoot/root ratio of concentration of As in *P. vittata* was much higher than that in *N. exaltata*, and was the highest (1.27) when exposed to 500 μ M As (Fig. 1).

Changes in the concentrations of LMWTs in *P. vittata* and *N. exaltata* grown with different concentrations of As were investigated. The concentrations of cysteine and γ EC in the shoots increased with increasing concentrations of As in the medium in both *P. vittata* and *N. exaltata* (Fig. 2). The concentrations of GSH in the shoots and roots of *P. vittata* also increased by As exposure, whereas the same decreased in *N. exaltata*, especially in the roots. The concentration of γ EC was very low compared to other LMWTs.

<Figs. 1&2

3.2. Experiment 2: Relationships between various oxidative stresses and low-molecular-weight thiol synthesis in *Pteris vittata*

Oxidative stress levels were estimated by lipid peroxidation in roots that directly received rhizosphere stresses (As, Cd, and H₂O₂). All treatments more or less increased the TBARS levels (lipid peroxidation) in roots, whereas the Cd and H₂O₂ treatments induced lipid peroxidation much earlier (Day 1) than As treatment (Day 3) (Fig. 3). In contrast, the LMWT concentrations in roots increased only by the As treatment.

<Fig. 3

3.3. Experiment 3: Expression analysis of arsenic related genes in *Pteris vittata*

Two putative γ ECS genes isolated by RT-PCR were named *PvECS1* and *PvECS2*. *PvECS1* consisted of 1965 bp, of which 1506 bp represent the open reading frame (ORF) encoding a protein of 502 amino acids, and *PvECS2* consisted of 1696 bp, of which 1317 bp represent the ORF encoding a protein of 439 amino acids (Figs. S2, S3). Both amino acid sequences were highly homologous to the γ ECS genes of *A. thaliana*, *B. juncea*, and *O. sativa* (Fig. S4A) with slight differences, particularly in the 3' region (Fig. S4B). These two genes belonged to the GCS2 (glutamate-cysteine ligase family 2) superfamily and are expected to have a functional role similar to γ ECS (EC : 6.3.2.2). Sequence data of *PvECS1* and *PvECS2* can be found in the EMBL/GenBank/DDBJ data libraries under accession numbers AB553576 (*PvECS1*) and AB553577 (*PvECS2*).

Temporal changes in the expression of genes following As exposure, which were expected to

impact As tolerance as well the concentrations of LMWT and As, were investigated. The expression patterns of *PvACR2* and *PvPCS* in response to As were similar (Fig. 4). Their expression increased at 12 h in roots, and thereafter at 48 h in shoots. The expression of *PvECS1* in shoots was repressed immediately by As exposure and remained low thereafter (Fig. 4). In contrast, the expression of *PvECS2* increased greatly after the 48-h treatment (Fig. 4). The expression pattern of *PvECS2* almost corresponded to the changes in γ EC and GSH concentrations in shoots after the 12-h treatment. Just before these increases, As accumulation in shoots began to increase (Fig. 4).

<Fig. 4

3.4. Experiment 4: Localization of arsenic and low-molecular-weight thiol

Fig. 5A indicates the As levels in each segment as well as large variations in the concentration of As among them. When comparing each pinna, As concentration was the highest in the apical pinna and decreased progressively in lower pinna positions. As concentration was very low in the midribs, and was the highest at the edge of one pinna. Although most veins showed low As accumulation, high concentrations of As were detected in the veins of the apical part. Localization of GSH and PC_2 showed trends similar to that of As (Fig. 5A). When determining the correlation between As and LMWT (GSH + PC_2) concentrations in segments, a significant positive correlation was observed (Fig. 5B).

Furthermore, cellular localization of GSH was investigated using MCB as a fluorescent probe.

Fluorescent intensity was higher in the cross-section of the midrib with As exposure, in the vascular bundle in particular (Fig. 6). In a cross-section of an apical pinna with As exposure, fluorescence intensity was extremely high at the edge as well as in the upper and lower epidermal cells (Fig. 6). In a cross-section of the root tip, GSH occurred throughout in the -As treatment but was localized in the central cylinder in the +As treatment (Fig. 6).

<Figs. 5&6

4. Discussion

LMWTs play important roles in tolerance to toxic minerals such as As in higher plants. Although direct detoxification of As by binding with LMWT in *P. vittata* was debated (Zhang et al., 2004; Cai et al., 2004), recent studies indicated the involvement of LMWT compounds and sulfur nutrition in As uptake and accumulation in this species (Vetterlein et al., 2009; Wei et al., 2010). Furthermore, it is possible that LMWTs contribute to the alleviation of oxidative stress induced by As. Hence, this study aimed to examine the relationship between As and LMWTs in detail.

First, the response of LMWT synthesis to As exposure in *P. vittata* was compared with that in *N. exaltata*. In contrast to *P. vittata*, *N. exaltata* is a non-As accumulator fern, and most As absorbed by roots remains in roots (Fig. 1). Concentrations of GSH in the roots of *N. exaltata* were higher than that of *P. vittata* in the absence of As, but decreased drastically with increasing As concentrations in the medium (Fig. 2). This decline may be due to the consumption of GSH without recovery for alleviating As stress. By contrast, GSH concentrations in *P. vittata* were drastically increased by As exposure, especially in shoots (Fig. 2). The results strongly suggest that LMWTs (e.g. GSH) are related to the different characteristics of As accumulation in fern species. Relatively high concentration of GSH did not lead to As hyperaccumulation in shoots in *N. exaltata* (Fig. 2), presumably indicating that cellular and/or subcellular localization of LMWTs (e.g. vacuole) would also be an important factor responsible for As hyperaccumulation in fern species.

Oxidative stress is a known primary factor contributing to As toxicity in plants, and LMWTs can alleviate the oxidative damage, as described before (Leustek et al., 1999; Requejo and Tena, 2005). Therefore, it is possible that the As-induced oxidative stress increases LMWT synthesis. To clarify whether LMWT synthesis in *P. vittata* is induced by As directly or indirectly via the As-induced oxidative stress, the effect of As, Cd, and H₂O₂ treatments on the induction of LMWT synthesis and lipid peroxidation was examined. Although all treatments induced oxidative stress in roots, only As exposure induced LMWT synthesis (Fig. 3) indicating that LMWT synthesis was not caused indirectly by oxidative stress but directly by As.

How does As affect the synthetic route for LMWTs? In general, γ EC synthesis is the rate-limiting factor in the pathway of GSH and PC syntheses (Tripathi et al., 2007). So, temporal changes in LMWT and As concentrations as well as in the expression of γ ECS gene following As exposure were investigated. Before this, the γ ECS gene in *P. vittata* was cloned. Two putative γ ECS genes (*PvECS1* and *PvECS2*) were isolated in this study. The expression pattern of these genes in response to As exposure differed entirely in *P. vittata* shoots (Fig. 4) in spite of their similar sequences (Fig. S4B). The As-induced increase in the *PvECS1* gene expression was not observed in shoots. The expression of *PvECS2* in shoots profoundly increased after As accumulation, and corresponded well to the increase in the concentration of GSH in shoots (Fig. 4). A delay in γ EC accumulation, the direct product of γ ECS, in shoots might have resulted from feedback inhibition of glutathione

synthetase by GSH (Fig. 4). Although *PvECS2* remains to be characterized, this gene might contribute to the As-specific induction of LMWT synthesis in *P. vittata*.

Finally, the localization of As and LMWT was compared at the whole-frond and cellular levels. When investigating the distribution of As and LMWT in the entire frond, As concentration was the highest in the apical pinna apex and decreased progressively in pinna at lower positions (Fig. 5A). Arsenic concentration was the highest at the edge in one pinna. These trends in distribution may result from transpiration. Interestingly, the localization of GSH and PC₂ showed similar trends to that of As (Fig. 5A). Furthermore, cellular localization of GSH was observed using cross-sections of pinnae and root tips. As observed for the whole shoot, a cross-section of the pinna indicated GSH localization in the edge of frond (Fig. 6). GSH was also localized in the epidermis (upper and lower) and vascular bundle (Fig. 6). Although we did not determine the cellular localization of As, a higher localization of As is reported in the epidermal cells (Lombi et al., 2002) and vascular bundles (Kitajima et al., 2008) in *P. vittata*. In consequence, As and LMWTs are colocalized in fronds at both whole-frond and cellular levels.

Then, what is the primary role(s) of LMWTs, specifically induced by As and colocalized with As? As described in the Introduction section, several possibilities with regard to the role of As in LMWT synthesis can be suggested. One is a defense to oxidative stress induced by As. In Experiment 2, As-induced lipid peroxidation in roots was delayed and milder in As exposed plants

compared with that in Cd and H₂O₂ (Fig. 3). This may be due to the alleviation of oxidative stress by newly synthesized LMWTs when exposed to As. Since glutathione reductase, which reduces oxidized glutathione (GSSG), is inactive in *P. vittata* (Kertulis–Tartar et al., 2009; Srivastava et al., 2005), *P. vittata* may adapt to As-induced oxidative stress by enhancing GSH synthesis. Cao et al. (2004) reported that not only the concentration of LMWTs but also the activity of enzymatic antioxidants (superoxide dismutase, catalase, ascorbate peroxidase, guaiacol peroxidase) were increased by As exposure in *P. vittata*. Thus, *P. vittata* is likely to resist As-induced oxidative stress comprehensively.

On the other hand, another idea that LMWTs are directly related to As tolerance by forming complexes cannot be dismissed. As(V) reductase and PC synthase are enzymes that mediate As(V) reduction and PC synthesis, respectively, and are involved in a series of reactions to detoxify As by forming As-LMWT complexes. Expression of the genes coding for these enzymes, *PvACR2* and *PvPCS*, was corresponded to As accumulation both in roots and shoots (Fig. 4). Moreover, significant positive correlation was observed when determining the correlation between As and LMWT (GSH + PC₂) concentrations in the segments in Experiment 4 (Fig. 5B). The regression line indicated the molar ratio of As : thiol group was ca. 1 : 2.97, which was nearly equal to the ideal molar ratio of As : thiol group when forming As-LMWT complexes in solution (1 : 3). These results support the hypothesis that As forms complexes with LMWTs in *P. vittata*. However, the 3

nonnegligible outliers lie away from the regression line (Fig. 5B). These outliers were obtained from segments in apical pinna that contained the highest As concentration among all the frond segments analyzed. This suggests that As–LMWT complexes are not the primary detoxified forms of As for storage in *P. vittata* because As : thiol group ratio was broken in the major accumulation site of As in a frond. Several previous reports also have negative results for direct detoxification of As by LMWTs. Raab et al. (2004) showed that the molar ratio of As–PC to total As was extremely low in *Pteris cretica* using HPLC-ICP-MS/ESI-MS system. Similarly, As–GS complexes were not detected in *P. vittata* fronds in the XANES analysis (Pickering et al., 2006). Meanwhile, it has been reported that GSH application enhances As uptake and translocation in *P. vittata*. LMWTs may not involved in direct As detoxification but partly contribute in transporting As to As-insensitive sites such as vacuoles to avoid toxic effects in the cytosol by temporarily forming complexes.

Acknowledgments

We are grateful to Dr Nobuyuki Kitajima, Fujita Corporation, who kindly provided *Pteris vittata* seedlings. This research was partly supported by the Kurita Water and Environment Foundation.

References

- Benavides, M.P., Gallego, S.M., Tomaro, M.L., 2005. Cadmium toxicity in plants. *Brazilian Journal of Plant Physiology* 17, 21-34.
- Bleeker, P.M., Hakvoort, H.W.J., Bliet, M., Souer, E., Schat, H., 2006. Enhanced arsenate reduction by a CDC25-like tyrosine phosphatase explains increased phytochelatin accumulation in arsenate-tolerant *Holcus lanatus*. *Plant Journal* 45, 917-929.
- Cai, Y., Su, J., Ma, L.Q., 2004. Low molecular weight thiols in arsenic hyperaccumulator *Pteris vittata* upon exposure to arsenic and other trace elements. *Environmental Pollution* 129, 69-78.
- Cao, X., Ma, L.Q., Tu, C., 2004. Antioxidative responses to arsenic in the arsenic-hyperaccumulator Chinese brake fern (*Pteris vittata* L.). *Environmental Pollution* 128, 317-325.
- Caille, N., Swanwick, S., Zhao, F.J., McGrath, S.P., 2004. Arsenic hyperaccumulation by *Pteris vittata* from arsenic contaminated soils and the effect of liming and phosphate fertilisation. *Environmental Pollution* 132, 113-120.
- Delnomdedieu, M., Basti, M.M., Otvos, J.D., Thomas, D.J., 1994. Reduction and binding of arsenate and dimethylarsinate by glutathione: a magnetic resonance study. *Chemico-Biological Interactions* 90, 139-155.
- Dhankher, O.P., Li, Y., Rosen, B.P., Shi, J., Salt, D., Senecoff, J.F., Sashti, N.A., Meagher, R.B.,

2002. Engineering tolerance and hyperaccumulation of arsenic in plants by combining arsenate reductase and γ -glutamylcysteine synthetase expression. *Nature Biotechnology* 20, 1140-1145.
- Dong, R., Formentin, E., Losseso, C., Carimi, F., Benedetti, P., Terzi, M., Schiavo, F.L., 2005. Molecular cloning and characterization of a phytochelatin synthase gene, *PvPCS1*, from *Pteris vittata* L. *Journal of Industrial Microbiology and Biotechnology* 32, 527-533.
- Ellis, D.R., Gumaelius, L., Indriolo, E., Pickering, I.J., Banks, J.A., Salt, D.E., 2006. A novel arsenate reductase from the arsenic hyperaccumulating fern *Pteris vittata*. *Plant Physiology* 141, 1544-1554.
- Francesconi, K., Visoottiviseth, P., Sridokchan, W., Goessler, W., 2002. Arsenic species in an arsenic hyperaccumulating fern, *Pityrogramma calomelanos*: a potential phytoremediator of arsenic-contaminated soils. *Science of Total Environment* 284, 27-35.
- Grill, E., Winnacker, E.-L., Zenk, M.H., 1985. Phytochelatin: The principal heavy-metal complexing peptides of higher plants. *Science* 230, 674-676.
- Hartley-Whitaker, J., Ainsworth, G., Meharg, A.A., 2001. Copper- and arsenate-induced oxidative stress in *Holcus lanatus* L. clones with differential sensitivity. *Plant, Cell & Environment* 24, 713-722.
- Kertulis, G.M., Ma, L.Q., MacDonald, G.E., Chen, R., Winefordner, J.D., Cai, Y., 2005. Arsenic

- speciation and transport in *Pteris vittata* L. and the effects on phosphorus in the xylem sap. *Environmental Experimental Botany* 54, 239-247.
- Kertulis-Tartar G.M., Rathinasabapathi, B., Ma, L.Q., 2009. Characterization of glutathione reductase and catalase in the fronds of two *Pteris* ferns upon arsenic exposure. *Plant Physiology and Biochemistry* 47, 960-965.
- Kitajima, N., Kashiwabara, T., Fukuda, N., Endo, S., Hokura, A., Nakai, Y.T.I., 2008. Observation of arsenic transfer in leaf tissue of hyperaccumulator fern by utilizing synchrotron radiation micro-XRF imaging. *Chemistry Letters* 37, 32-33.
- Leustek, T., Saito, K., 1999. Sulfate transport and assimilation in plants. *Plant Physiology* 120, 637-644.
- Li, Y., Dankher, O.P., Carreira, L., Smith, A.P., Meagher, R.B., 2006. The shoot-specific expression of gamma-glutamylcysteine synthetase directs the long-distance transport of thiol-peptides to roots conferring mercury and arsenic. *Plant Physiology* 141, 288-298.
- Lombi, E., Zhao, F.-J., Fuhrmann, M., Ma, L.Q., McGrath, S.P., 2002. Arsenic distribution and speciation in the fronds of the hyperaccumulator *Pteris vittata*. *New Phytologist* 156, 195-203.
- Ma, L.Q., Komar, K.M., Tu, C., Zhang, W., Cai, Y., Kennelley, E.D., 2001. A fern that hyperaccumulates arsenic. *Nature* 409, 579.

- Pickering, I.J., Gumaelius, L., Harris, H.H., Prince, R.C., Hirsch, G., Banks, J.A., Salt, D.E., George, G.N., 2006. Localizing the biochemical transformations of arsenate in a hyperaccumulating fern. *Environmental Science & Technology* 40, 5010-5014.
- Raab, A., Feldmann, J., Meharg, A.A., 2004. The nature of arsenic-phytochelatin complexes in *Holcus lanatus* and *Pteris cretica*. *Plant Physiology* 134, 1113-1122.
- Requejo, R., Tena, M., 2005. Proteome analysis of maize roots reveals that oxidative stress is a main contributing factor to plant arsenic toxicity. *Phytochemistry* 66, 1519-1528.
- Schützendübel, A., Nikolova, P., Rudolf, C., Polle, A., 2002. Cadmium and H₂O₂-induced oxidative stress in *Populus × canescens* roots. *Plant Physiology and Biochemistry* 40, 577-584.
- Shri, M., Kumar, S., Chakrabarty, D., Trivedi, P.K., Mallick, S., Misra, P., Shukla, D., Mishra, S., Srivastava, S., Tripathi, R.D., Tuli, R., 2009. Effect of arsenic on growth, oxidative stress, and antioxidant system in rice seedlings. *Ecotoxicology and Environmental Safety* 72, 1102-1110.
- Singh, N., Ma, L.Q., Srivastava, M., Rathinasabapathi, B., 2006. Metabolic adaptations to arsenic-induced oxidative stress in *Pteris vittata* L and *Pteris ensiformis* L. *Plant Science* 170, 274-282.
- Sneller, F.E.C., van Heerwaarden, L.M., Koevoets, P.L.M., Vooijs, R., Schat, H., Verkleij, J.A.C., 2000. Derivatization of phytochelatin from *Silene vulgaris*, induced upon exposure to

- arsenate and cadmium: Comparison of derivatization with Ellman's reagent and monobromobimane. *Journal of Agricultural and Food Chemistry* 48, 4014-4019.
- Srivastava, M., Ma, L.Q., Singh, N., Singh, S., 2005. Antioxidant responses of hyper-accumulator and sensitive fern species to arsenic. *Journal of Experimental Botany* 56, 1335-1342.
- Srivastava, S., Srivastava, A.K., Suprasanna, P., D'Souza, S.F., 2010. Comparative biochemical and transcriptional profiling of two contrasting varieties of *Brassica juncea* L. in response to arsenic exposure reveals mechanisms of stress perception and tolerance. *Journal of Experimental Botany* (in press).
- Tripathi, R.D., Srivastava, S., Mishra, S., Singh, N., Tuli, R., Gupta, D.K., Maathuis, F.J.M., 2007. Arsenic hazards: strategies for tolerance and remediation by plants. *Trends in Biotechnology* 25, 158-165.
- Ullrich-Eberius, C.I., Sanz, A., Novacky, A.J., 1989. Evaluation of arsenate- and vanadate-associated changes of electrical membrane potential and phosphate transport in *Lemna gibba* G1. *Journal of Experimental Botany* 40, 119-128.
- Vetterlein, D., Wesenberg, D., Nathan, P., Bräutigam, A., Schierhorn, A., Mattusch, J., Jahn, R., 2009. *Pteris vittata*-revisited: Uptake of As and its speciation, impact of P, role of phytochelatins and S. *Environmental Pollution* 157, 3016-3024.
- Wang, J., Zhao, F.-J., Meharg, A.A., Raab, A., Feldmann, J., McGrath, S.P., 2002. Mechanisms of

arsenic hyperaccumulation in *Pteris vittata*. Uptake kinetics, interactions with phosphate, and arsenic speciation. *Plant Physiology* 130, 1552-1561.

Watanabe, T., Broadley, M.R., Jansen, S., White, P.J., Takada, J., Satake, K., Takamatsu, T., Tuah, S.J., Osaki, M., 2007. Evolutionary control of leaf element composition in plants. *New Phytologist* 174, 516-523.

Wei, S., Ma, L.Q., Saha, U., Mathews, S., Sundaram, S., Rathinasabapathi, B., Zhou, Q., 2010. Sulfate and glutathione enhanced arsenic accumulation by arsenic hyperaccumulator *Pteris vittata* L. *Environmental Pollution* 158, 1530-1535.

Zhang, W., Cai, Y., Downum, K.R., Ma, L.Q., 2004. Thiol synthesis and arsenic hyperaccumulation in *Pteris vittata* (Chinese brake fern). *Environmental Pollution* 131, 337-345.

Zhao, F.J., Wang, J.R., Barker, J.H.A., Schat, H., Bleeker, P.M., McGrath, S.P., 2003. The role of phytochelatins in arsenic tolerance in the hyperaccumulator *Pteris vittata*. *New Phytologist* 159, 403-410.

Figure captions

Figure 1 Arsenic concentration in shoots and roots of *P. vittata* and *N. exaltata* exposed to 0, 100, and 500 μM As(V) for three days. Bars represent $\pm\text{SEs}$. Different text indicates statistically significant differences between species (indicated in upper case) or treatments (indicated in lower case) ($P < 0.05$).

Figure 2 Effect of different levels of As exposure on concentrations of Cys, γEC , and GSH in *P. vittata* and *N. exaltata*. Fern seedlings were exposed to 0, 100, and 500 μM As(V) for 3 days. Bars represent $\pm\text{SEs}$. Different text indicate statistically significant differences between treatments ($P < 0.05$). The concentrations of γEC in roots were below the detection limit.

Figure 3 Effects of various abiotic stresses (100 μM As, 50 μM Cd, 1 mM H_2O_2 , and control) on TBARS and total thiol concentrations in *P. vittata* roots. Total thiol was calculated by summing the concentrations of thiol in Cys, γEC , and GSH. Vertical bars indicate mean $\pm\text{SE}$.

Figure 4 Changes in concentrations of As (A), Cys (B), γEC (C), and GSH (D), and relative expression of *PvACR2* (E), *PvPCS* (F), *PvECS1*, and *PvECS2* (G) in *P. vittata* fronds. Fronds were sampled at 0, 0.5, 1, 5, 12, 24, 48, and 72 h after the onset of the As exposure. Gene expressions

were normalized relative to elongation factor-1b mRNA content.

Figure 5 Relationship among As, GSH, and PC₂ accumulations in *P. vittata* fronds. localization of As, GSH, and PC₂ in a frond (A); and correlation between As and thiols (GSH + PC₂) (B). The regression line was calculated using the concentrations in each segment with an As concentration of <math><20 \mu\text{mol g}^{-1}</math>. The region numbers in A are corresponded to the dot numbers in B.

Figure 6 Distribution of GSH in a cross-section of a frond (midrib and edge of pinna) and root tip of *P. vittata* grown with or without As. GSH in the sections was labeled with the fluorescence probe MCB. Light microscope images are also shown for each section.

Supplemental Data

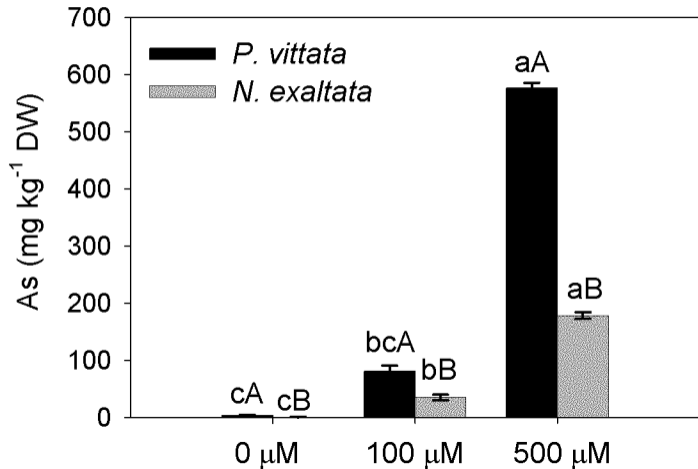
Figure S1 HPLC chromatograms showing the influence of the presence of the frond midribs on the detection of GSH, γ EC, and PC₂.

Figure S2 Base sequences of *PvECS1* and estimated amino acid sequences obtained from cDNA of *P. vittata*. The underlined text indicates the primer used for cloning, and the blue text indicates the primer used for real-time PCR. Untranslated region is indicated in lower case.

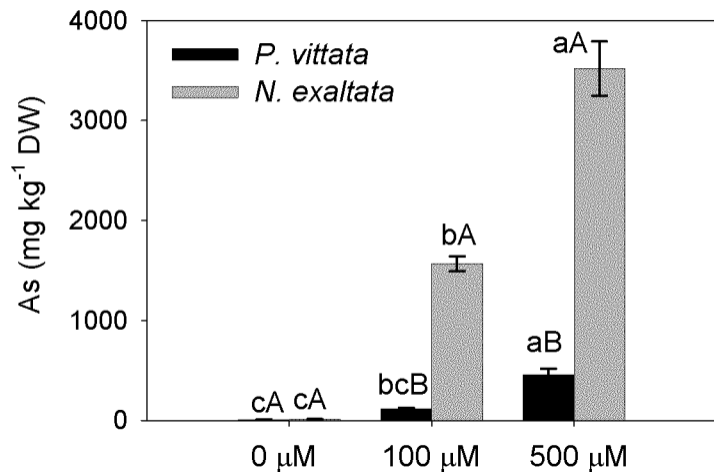
Figure S3 Base sequences of *PvECS2* and estimated amino acid sequences obtained from cDNA of *P. vittata*. The underlined text indicates the primer used for cloning, and the blue text indicates the primer used for real-time PCR. Untranslated region is indicated in lower case.

Figure S4 Alignment of the predicted amino acid sequences of *A. thaliana* (EMBL/GenBank/DBJ accession number: AJ508916), *B. juncea* (AJ563922), *O. sativa* (AJ508916), and *P. vittata* (PvECS1 and PvECS2) for the protein of γ ECS (A), and the extracted terminal sequences of PvECS1 and PvECS2 for comparison (B).

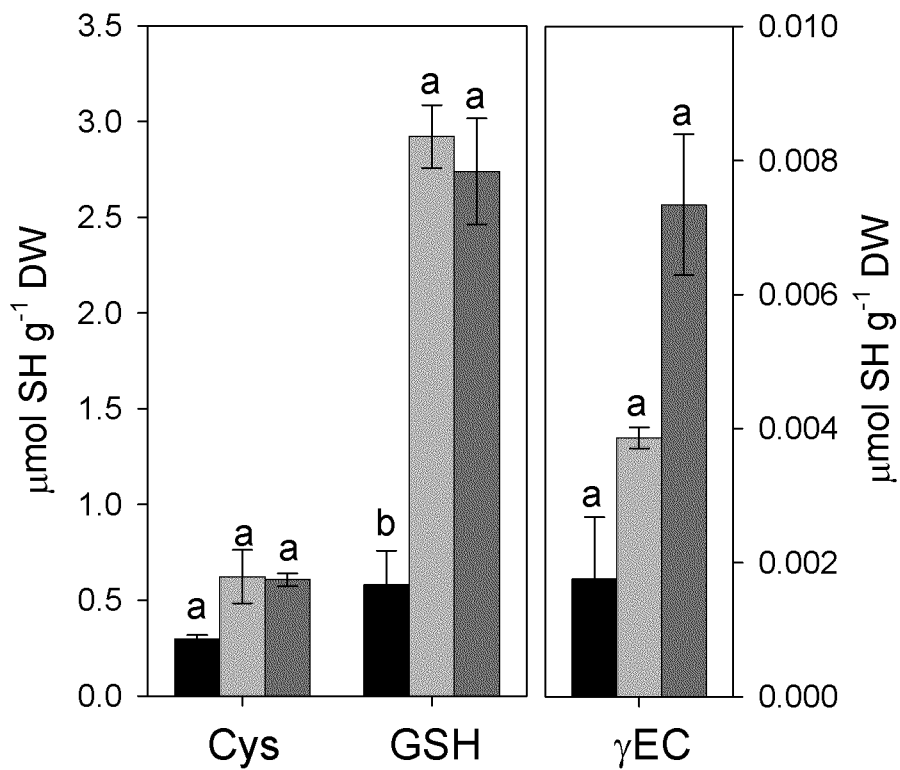
Shoot



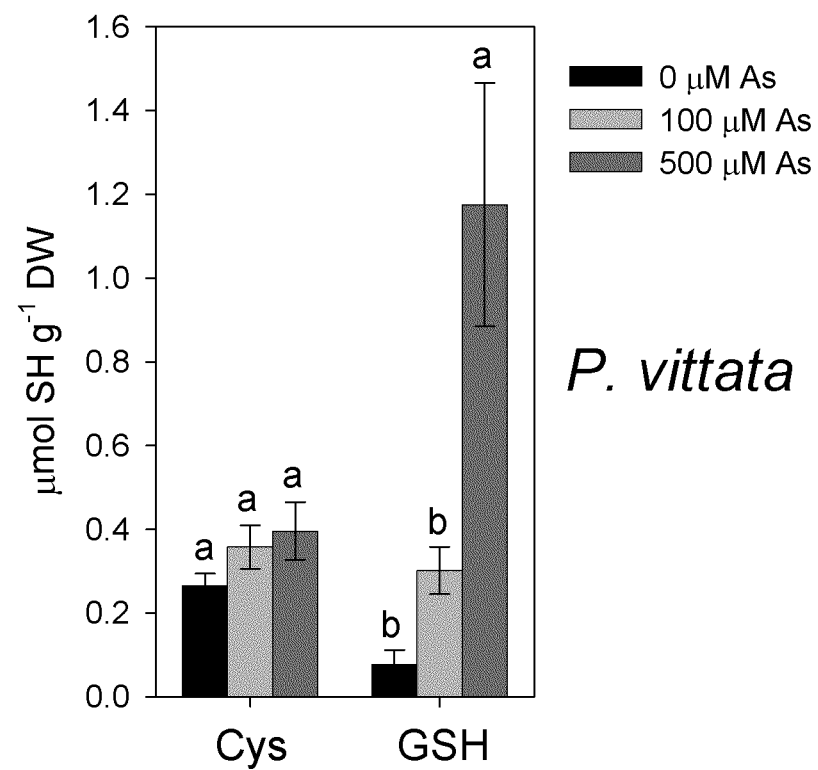
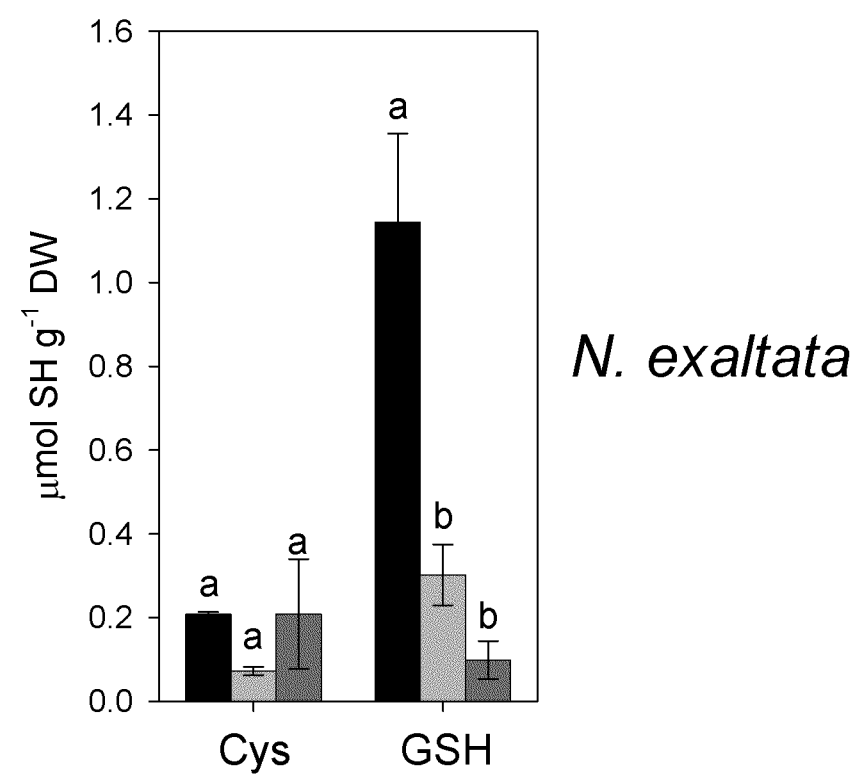
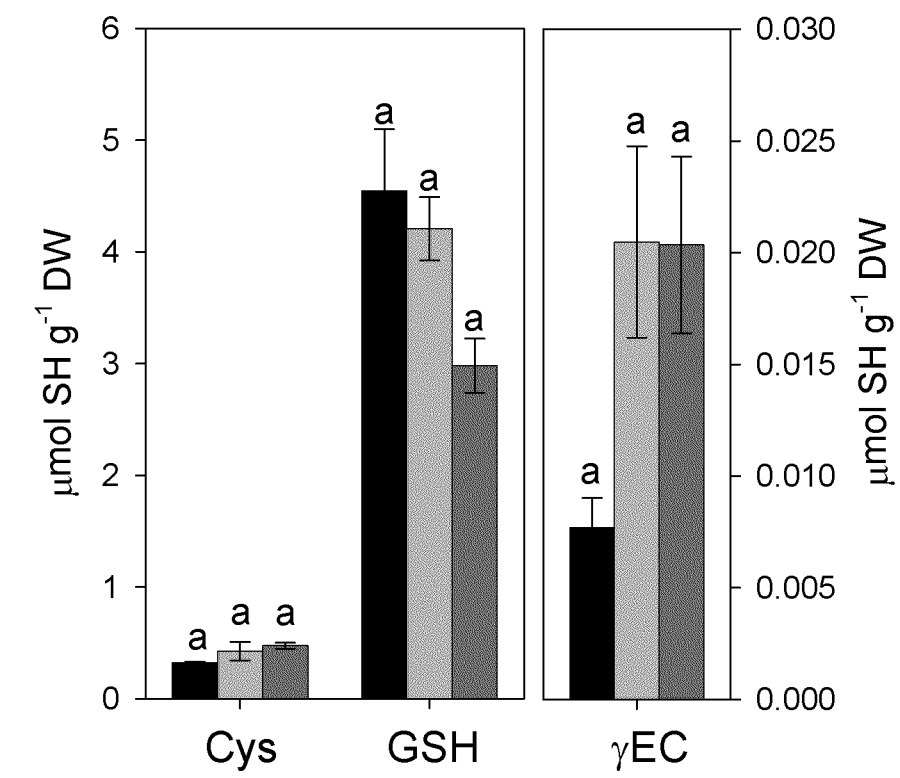
Root

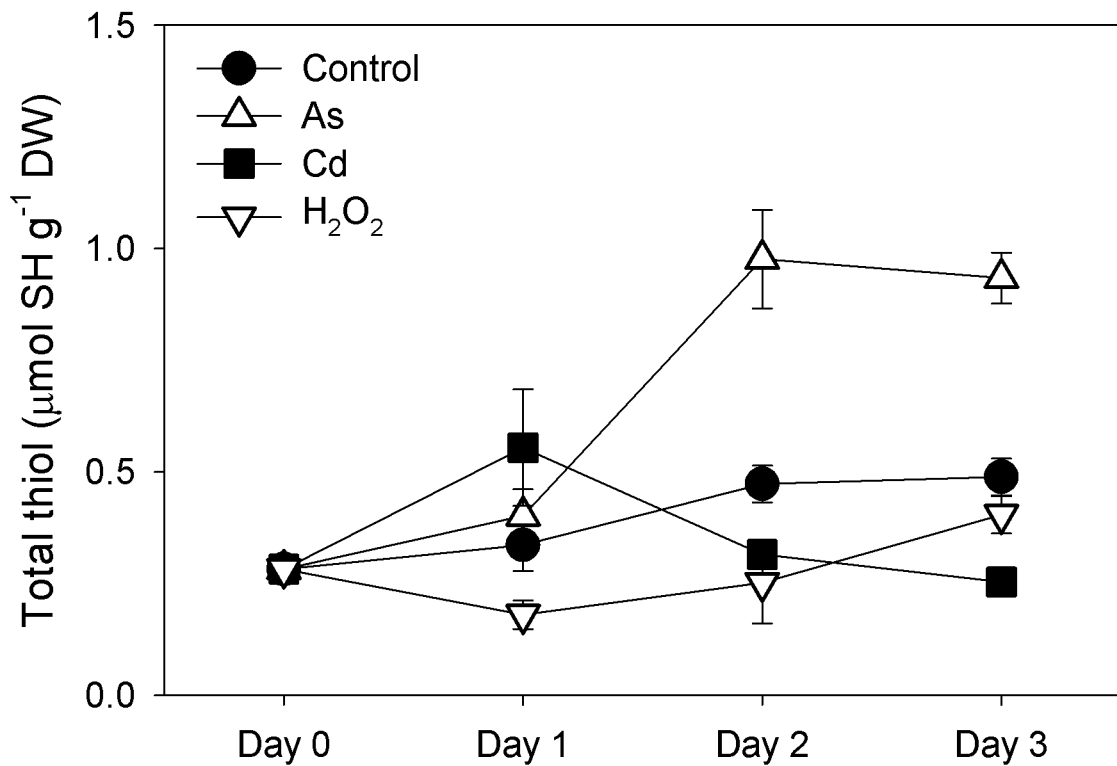
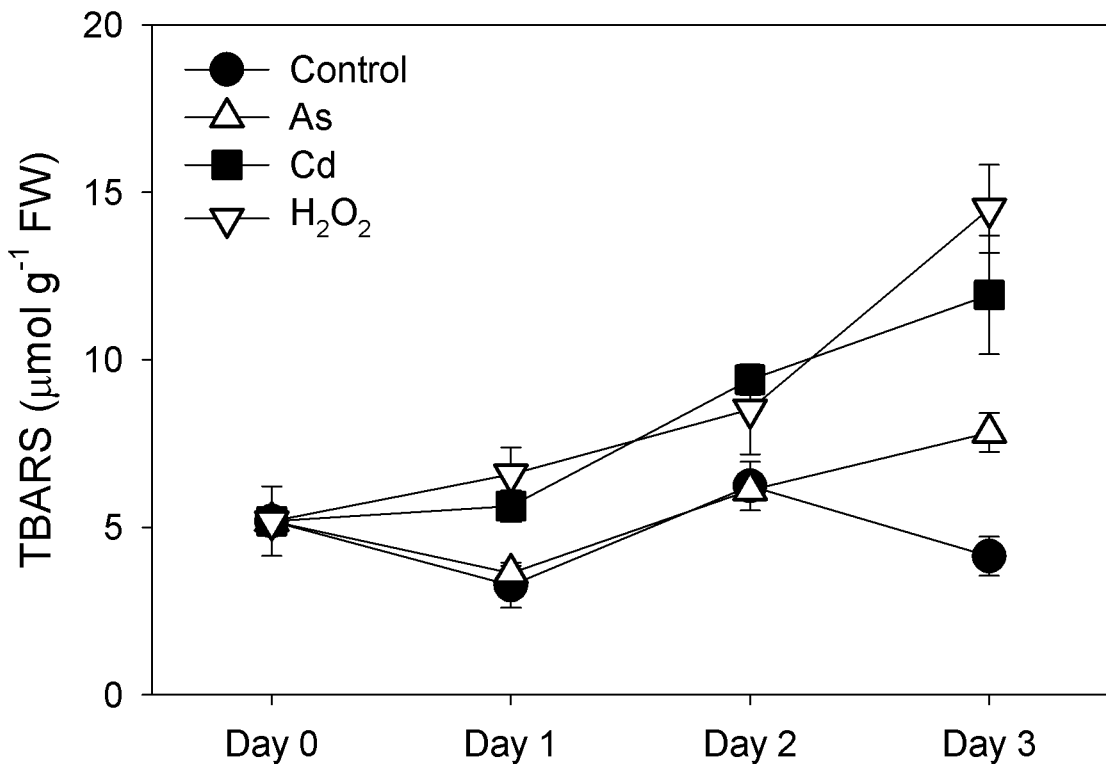


Shoot

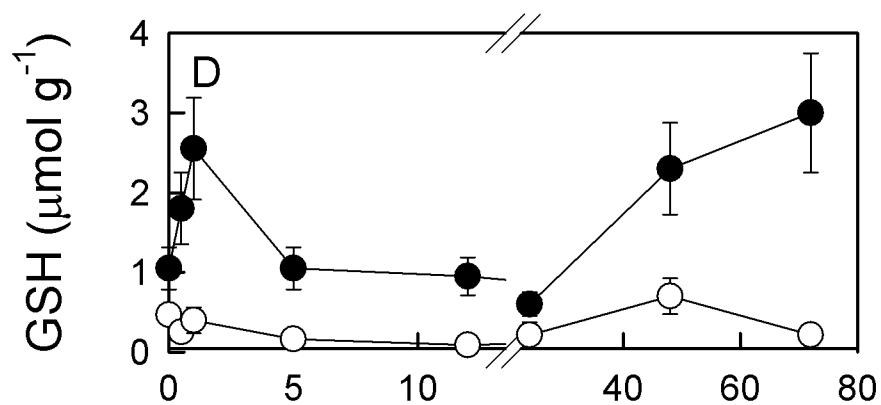
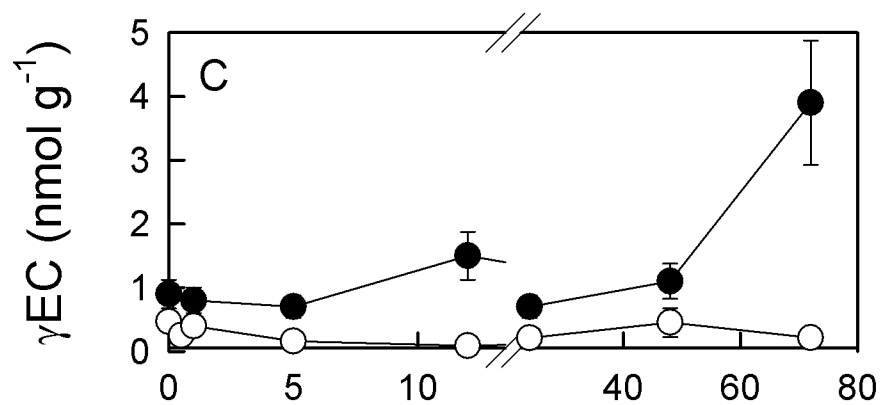
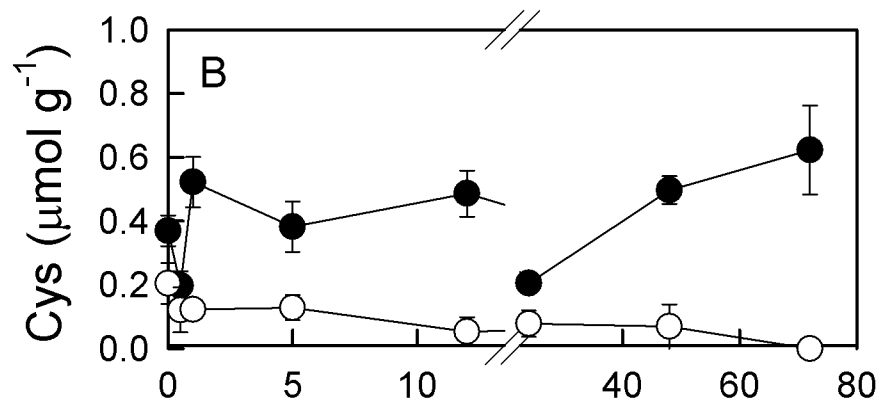
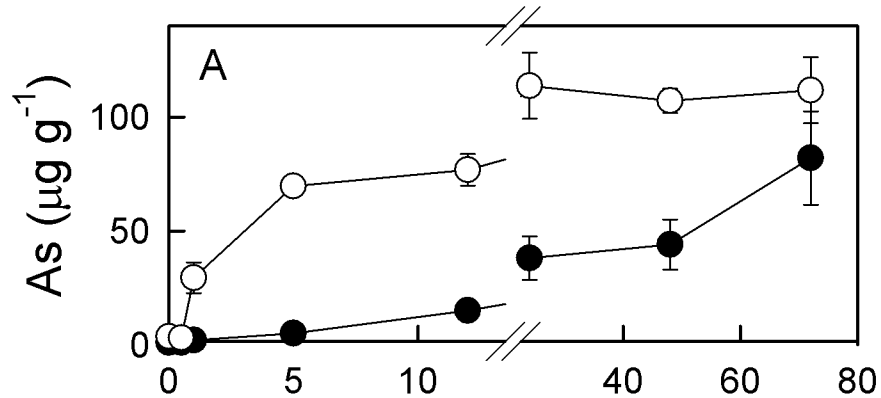


Root

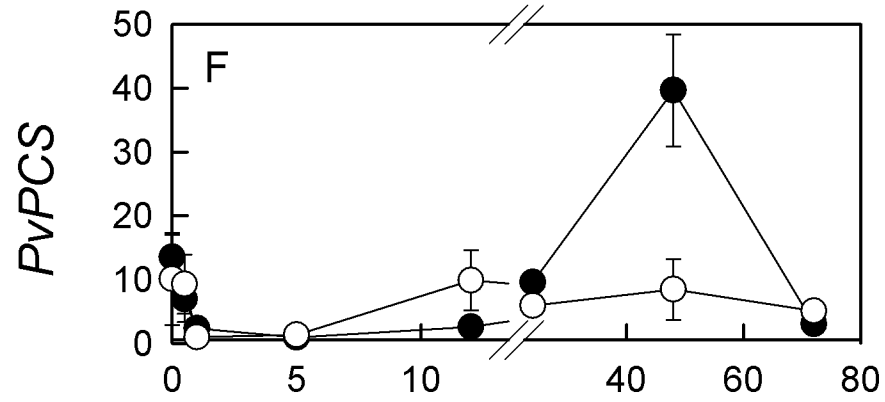
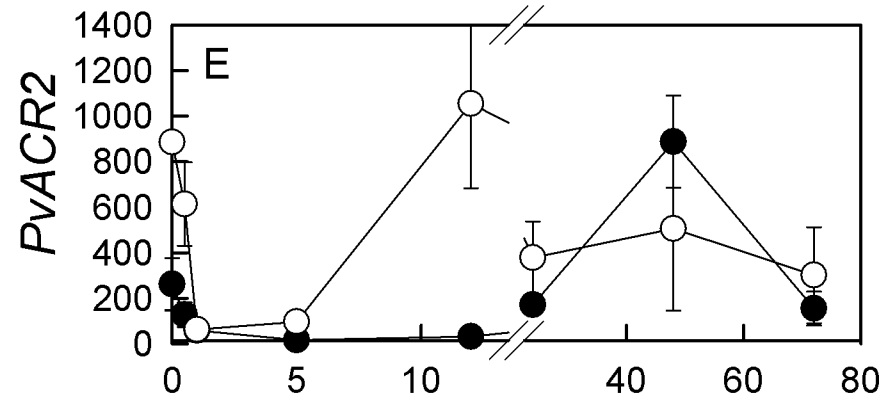
*P. vittata**N. exaltata*



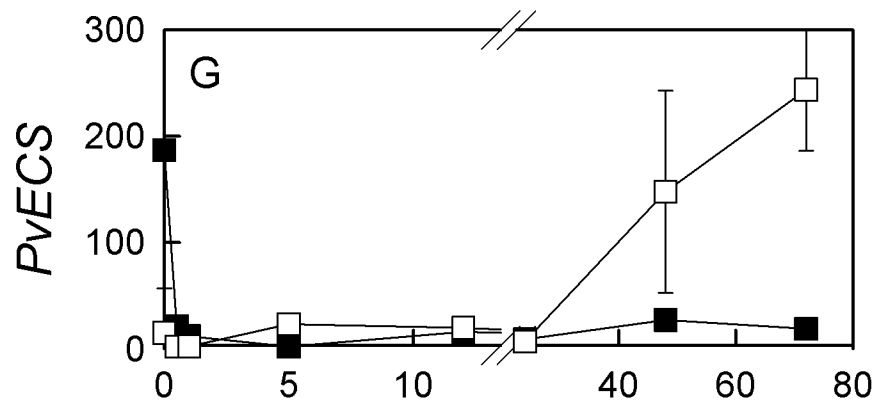
Concentration



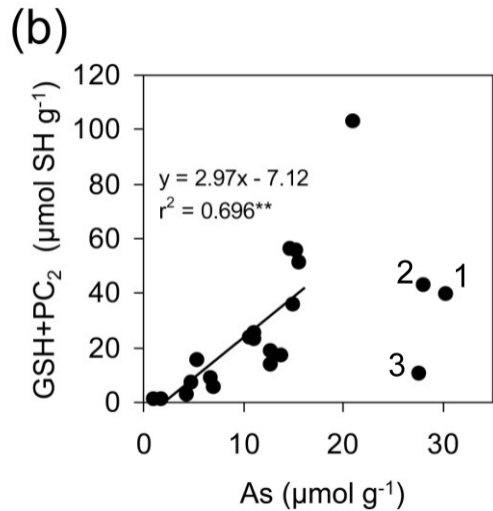
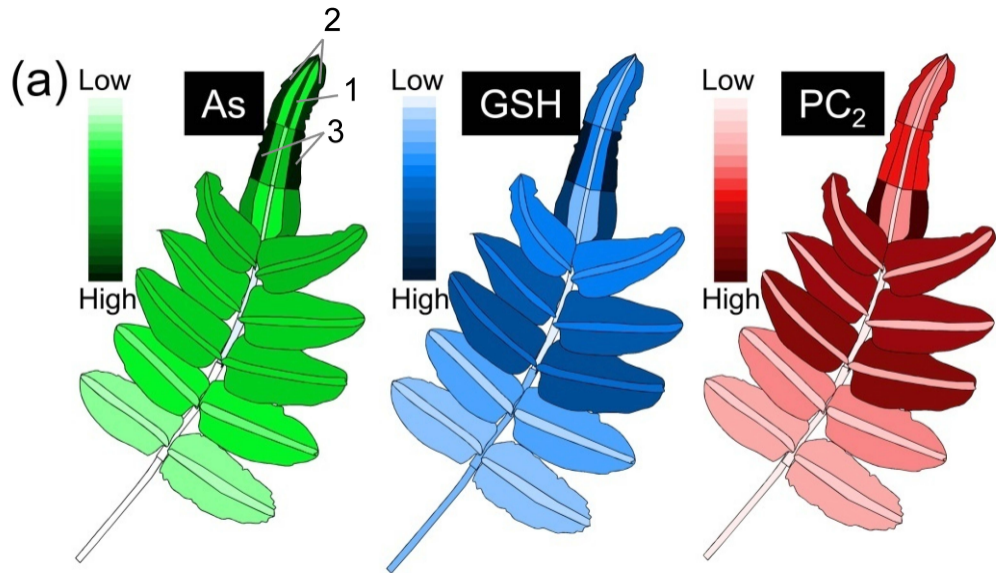
Relative expression



● Shoot
○ Root



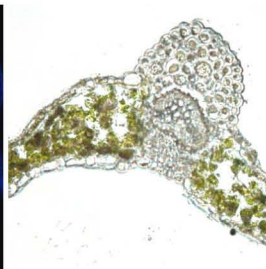
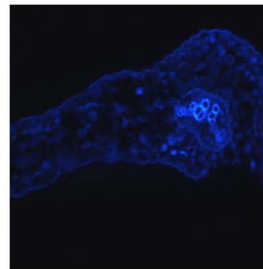
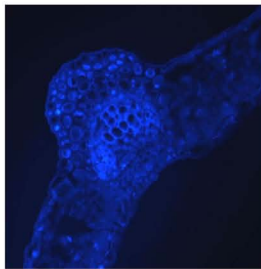
■ *PvECS1* in Shoot
□ *PvECS2* in Shoot



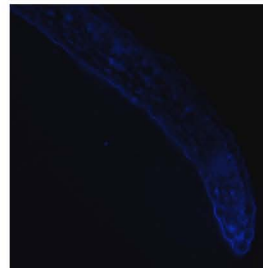
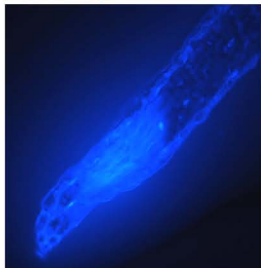
+As

-As

Midrib



Edge of pinna



Root tip

